JTTEE5 12:282-289

Splat Microstructure of Plasma Sprayed Cast Iron With Different Chamber Pressures

M.F. Morks, Y. Tsunekawa, M. Okumiya, and M.A. Shoeib

(Submitted 9 September 2001; in revised form 28 February 2002)

Achieving a plasma sprayed cast iron coating containing graphite requires stringent control on spray parameters that synergistically influence the coating properties and thus the performance. The microstructure of cast iron splats greatly depends on spray parameters such as substrate temperature, chamber pressure, and spray distance. This paper presents the effect of chamber pressure on the splat microstructure, including oxides and graphite. At low chamber pressures, most splats exhibit a disk shape with high flattening ratios, whereas star-shaped splats extensively appear at high chamber pressures. Spraying at high chamber pressures causes the formation of pores and thick oxide zones at the splat/substrate interface, mainly due to the atmospheric gases, which are responsible for a decrease in splat adhesion. Spraying in Ar atmosphere reduces the splat oxidation due to a decrease in the oxygen partial pressure. Small deformed substrate ridges are observed adjacent to the periphery of splats sprayed at low chamber pressures whereas no ridges are detected at high chamber pressures. Ridge formation generates a kind of mechanical bond, which increases the adhesive strength. Since the molten droplets impinge with high velocity and thus high flattening ratio at low chamber pressures, the solidification rate becomes faster, and graphite formation is resultantly hindered.

Keywords cast iron, chamber pressure, graphite, microstructure, oxidation, plasma spraying, splat morphology

1. Introduction

There is increasing worldwide interest in using aluminum alloys as base materials for many industrial applications, one such being in automotive cylinder blocks. These alloys have two outstanding properties: high thermal conductivity and low density. However, they exhibit poor anti-wear properties due to their softness, so surface modification is required for high load bearing applications. Recently, some methods have been successfully applied to improve the anti-wear property of cast aluminum alloy cylinder blocks.[1-3] Besides these methods, a superior wear-resistant surface can be achieved by cast iron coatings. That is because cast iron exhibits superior wear resistance arising from the self-lubricating property of graphite. However, graphite formation during plasma spraying of cast iron requires great care in the optimization of spray parameters that influence the solidification rate and thus the performance, since a sprayed cast iron coating generally contains carbides instead of graphite.[4]

The solidification rate of individual molten droplets impinged and flattened on a substrate affects properties of plasma sprayed coatings.[5] The microstructure of cast iron splats is linked to the solidification rate, which has a direct relationship with spray parameters such as substrate temperature, chamber pressure and spray distance. A good understanding of these parameters is achieved by studying their effect on the morphology, microstructure, interfacial reaction, and graphitization of individual splats. In our previous work,[6] the preheat substrate temperature was found to have a great effect on the morphology and microstructure of cast iron splats.

Sodeoka et al. have reported that higher chamber pressures cause the droplet velocity to slow down.[7] However, it has almost no effect on droplet temperatures at a certain spray distance. Fantassi et al. found that the flattening time decreases with increasing particle velocity but increases with particle size.[8] Some other related studies focused on the effect of oxidation on the splat morphology. The presence of dissolved oxygen in a solidifying splat affects the splat-substrate wetting, which in turn influences the splat flattening.[9-11] Several other studies have also reported on the influence of spray parameters such as chamber pressure on the splat morphology.[12-14]

The current study deals with the behavior of sprayed cast iron splats as a fundamental aspect of cast iron coatings containing graphite on an aluminum alloy substrate. The focus is on the effect of chamber pressure not only on the formation of pores and oxides, which strongly affect the adhesion, but also on the

Table 1 Spray Parameters for the Splat Collection on a Preheated Substrate at Different Chamber Pressures

Primary plasma gas	Ar, 0.0327 l/min
Secondary plasma gas	H_2, 0.00327 l/min
Arc current	500 A
Arc voltage	45 V
Powder carrier gas	Ar, 0.0017 l/min
Chamber pressure	26.3-100 kPa
Spray distance	350 mm
Substrate temperature	473 K
Spray material	Cast iron $38 < d_P < 45$ μM

M.F. Morks, Y. Tsunekawa, and **M. Okumiya,** Toyota Technological Institute, Nagoya, Japan; and **M.A. Shoeib,** Central Metallurgical Research and Development Institute, Cairo, Egypt. Contact e-mail: tsunekawa@toyota-ti.ac.jp.

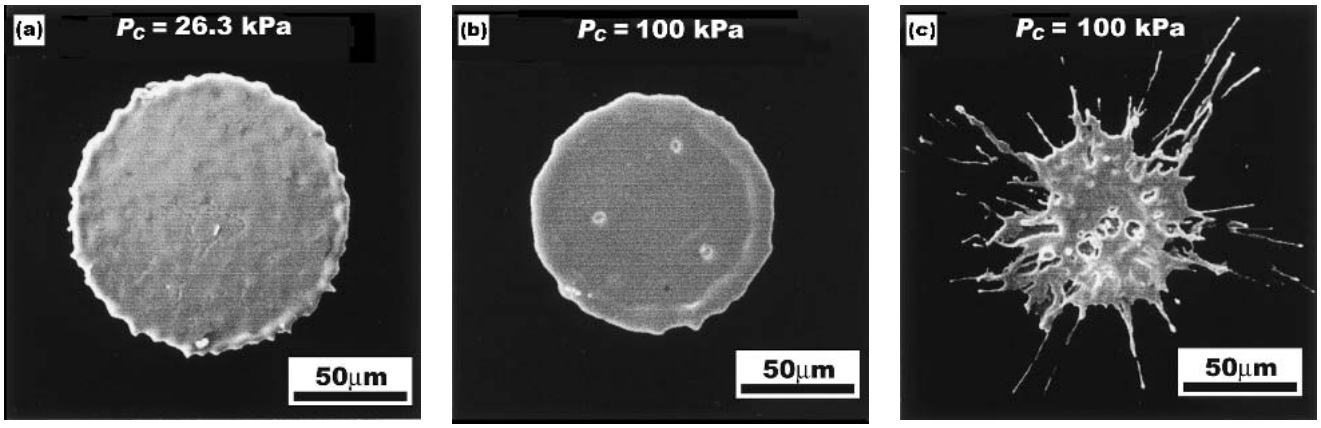

Fig. 1 SEM micrographs showing a splat morphology of cast iron sprayed at different P_C in Ar atmosphere

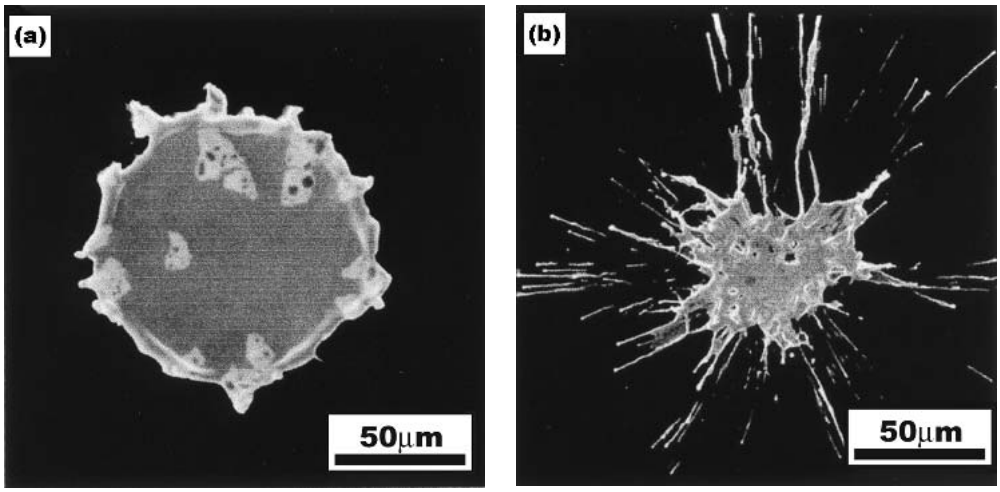

Fig. 2 SEM micrographs showing a splat morphology of cast iron sprayed at P_C = 100 kPa in air atmosphere: **(a)** disk and **(b)** star-shape

splat microstructure including graphitization, considering that chamber pressure plays a significant role in splat solidification through a change in the droplet velocity.

2. Experimental Procedures

A gas-atomized cast iron powder with chemical composition of Fe-3.75 C-2.70 Si-0.70 Mn-1.18 Al (all compositions in weight percent) was sieved into particle sizes (d_P) of 38-45 μm and fed into the plasma flame as a spray material, under spray parameters listed in Table 1. Cast iron droplets sprayed at a constant spray distance (d_S) of 350 mm were collected on a mirror-polished Al-Si-Cu alloy substrate for different chamber pressures (P_C). The preheat substrate temperature (T_S) was kept constant at 473 K for all splat collections and continuously recorded by keeping the thermocouple in contact with the substrate center.

To study the effect of P_C on the splat microstructure, several tens of molten droplets having a nearly equal temperature and velocity just before impinging were collected on a preheated substrate by passing through a masking plate with a circular hole

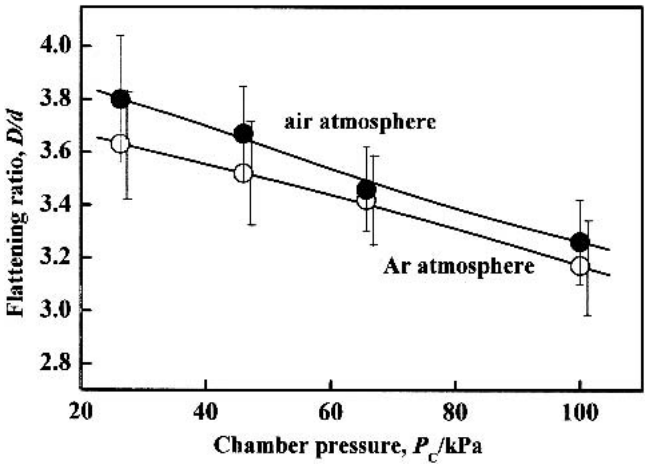

Fig. 3 Change in flattening ratio of cast iron disk splats as a function of P_C in Ar and air atmosphere

of 30 mm behind a moving graphite shutter. One series of spraying experiments has been carried out in Ar atmosphere by evacuating the chamber to 1.9 kPa before allowing the primary plasma

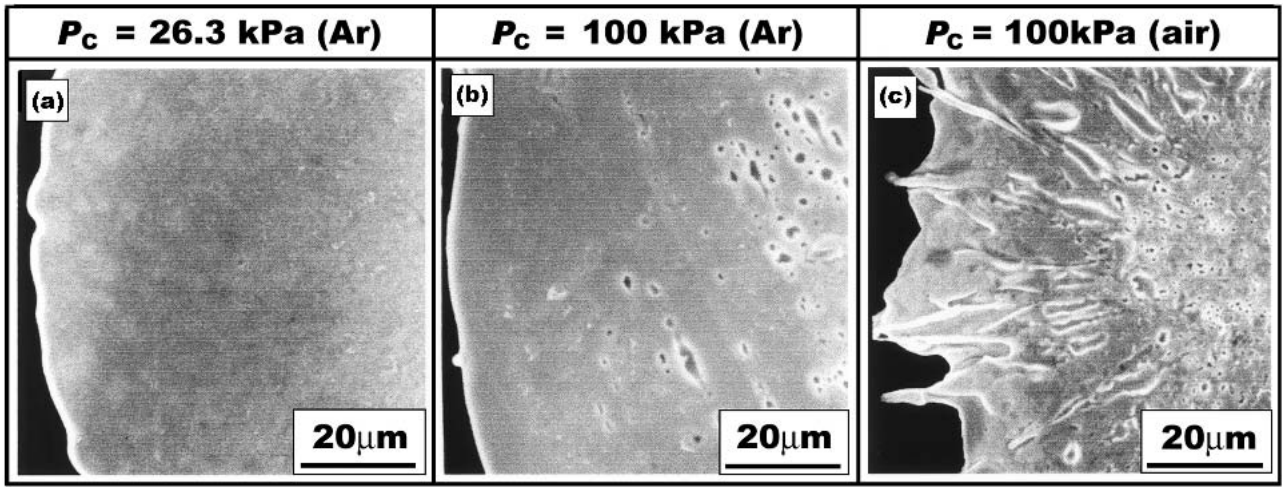

Fig. 4 Typical rear-side views of removed cast iron splats sprayed at different P_C

gas (Ar) to pass through the evacuated chamber to the operating P_C. The other series of sprayings was achieved by evacuating the chamber exactly to the operating P_C. In the extreme case spraying was achieved in air atmosphere at 100 kPa. These kinds of experiments help us examine the effect of oxygen partial pressure on the microstructure and oxidation of cast iron splats. In spite of its inapplicable to automotive cylinder bore surfaces, spraying in a chamber at different P_C provides important information about the sensitivity of cast iron droplets for oxidation and graphite formation at a given spray distance. Cast iron coatings containing graphite are quite effective for achieving a low friction coefficient for other aluminum components with severe sliding areas.

The number fraction of each splat morphology, i.e., disk and star-shaped splats sprayed at different P_C, was calculated by counting the corresponding splats using an optical microscope. Using a conductive adhesive tape, mainly composed of carbon, to remove splats from the substrate surface makes it feasible to examine the pore formation on the rear-side. The number fraction of removed splats was simultaneously counted to make an approximate evaluation of the adhesive property of splats sprayed at different P_C.

Splat cross-sections were carefully prepared to examine the splat/substrate interface. The samples were polished with emery papers and then buff-polished with dilute aqueous Al_2O_3 powder slurry. After rinsing with water and C_2H_5OH, the cross-sections were etched for 5-60 s by nital. The topside of cast iron splats was gently buffed with dilute aqueous Al_2O_3 powder slurry and etched to clarify the microstructure of splats, especially the graphite and Fe_3C formation. Element analyses on the cross-section and the topside of splats have been performed by an electron probe microanalyzer (EPMA). Different phases of splats were identified by x-ray diffractometry (XRD) with Co K_α radiation.

3. Results and Discussion

3.1 Splat Morphology

Typical morphologies of cast iron splats sprayed at P_C of 26.3 kPa, 100 kPa in Ar, and 100 kPa in air atmosphere are shown in Fig. 1 and 2, respectively. Looking at Fig. 1, splats sprayed in Ar atmosphere at low P_C are characterized by a thin disk shape with a regular outer periphery (Fig. 1a), but those sprayed at high P_C are characterized by a relatively thick disk (Fig. 1b) as well as by a star shape (Fig. 1c). However, disk splats sprayed in air atmosphere exhibit white areas with irregular outer peripheries (Fig. 2a). The irregularity of the disk splats may be attributed to the formation of those white zones, which are identified as oxides as will be discussed later. Splat morphology is closely related to P_C, as confirmed by the classification into disk and star-shaped splats. Most splats exhibit a disk shape at low P_C. In contrast, the number fraction of star-shaped splats intensively increases with P_C regardless of spraying in Ar or air atmosphere, and no splashed splats appear in the spray conditions used in this study. A change in the splat morphology from disk to star-shaped splats with P_C is partially caused by the droplet velocity. Sodeoka et al. measured the droplet velocity at low and high P_C.[7] They have reported that the droplet velocity increases at low P_C. According

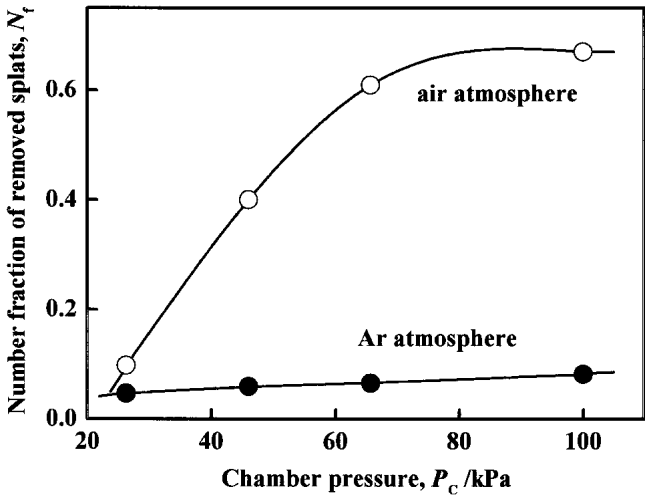

Fig. 5 Change in number fraction of removed cast iron splats as a function of P_C in Ar and air atmosphere

to the splat classification, disk splats intensively appear upon impinging of high velocity molten droplets at low P_C. Deformation dynamics of molten droplets on a substrate surface is affected by the interface condition. One important factor is wetting at the interface, which has an influence on the development of the contact between the lower surface of the spreading droplet and substrate surface.[15] The larger the contact angle, the harder the spreading. It seems that high surface tension at low temperatures restrains the droplets from extreme spreading with a disk shape. At low surface tension, the droplet extremely flattened and star-shaped splats appear due to the local difference in surface tension and viscosity.

The flattening ratio (D/d) of disk splats sprayed at different P_C in Ar and air atmosphere was calculated by measuring the splat diameter (D) and the molten droplet diameter (d) as a function of P_C, as described in Fig. 3. The diameter (d) was calculated by droplet volume on the premise of no-weight change in solid and liquid state.

The D/d ratio decreases with P_C due to a decrease in the velocity of molten droplets at impact on a substrate. However, they are slightly higher for splats sprayed in air atmosphere. It seems that droplets in air atmosphere have velocities a little higher than those in Ar atmosphere due to a difference in the viscosity of the atmosphere. At low P_C, the velocity of impinging droplets is high enough to make them expand widely on a substrate.[7] MacPherson reported that, if spreading is complete before solidification, the D/d ratio can be calculated from Madejiski's analysis using the following simplified equation[9]

$$D/d = 1.2941(\rho v d/\mu)^{0.2} \quad \text{(Eq 1)}$$

where v is the impact velocity, ρ the density, and μ the dynamic viscosity. The simple expression of Eq 1 shows the dependence of velocity of molten droplets on the D/d ratio.

3.2 Splat Adhesion

A conductive adhesive tape was used to remove splats from the substrate surface to reveal their rear-side appearance. The rear-side views of cast iron disk splats sprayed at 26.3 kPa in Ar, and at 100 kPa in Ar and air atmosphere are shown in Fig. 4. The pictures give an impression that the number of pores increases with P_C. However, splats sprayed at high P_C in Ar atmosphere (Fig. 4b) reveal a lesser number of pores than those sprayed in air atmosphere (Fig. 4c). At low P_C, the presence of small amounts of gases inside the chamber and at the substrate surface decreases the possibility of gas absorption and adsorption during the flight and flattening of droplets. Another reason is an increase in the droplet velocity at low P_C, which creates good wetting of droplets with the substrate upon impinging; that is, the strong impingement draws away gases at the interface and thus fewer numbers of pores appear. Poor wettability in air atmosphere also brings higher amounts of pores at the interface. From the rear-side observation of disk splats in our previous work,[6] there exist a few small pores at higher preheat substrate temperatures, which indicates good wetting between the splat and the substrate.

Approximate evaluation of the adhesive strength of splats sprayed at different P_C in Ar and air atmosphere was performed by measuring the number fraction of splats removed by an adhesive tape, as illustrated in Fig. 5. For splats sprayed in Ar at-

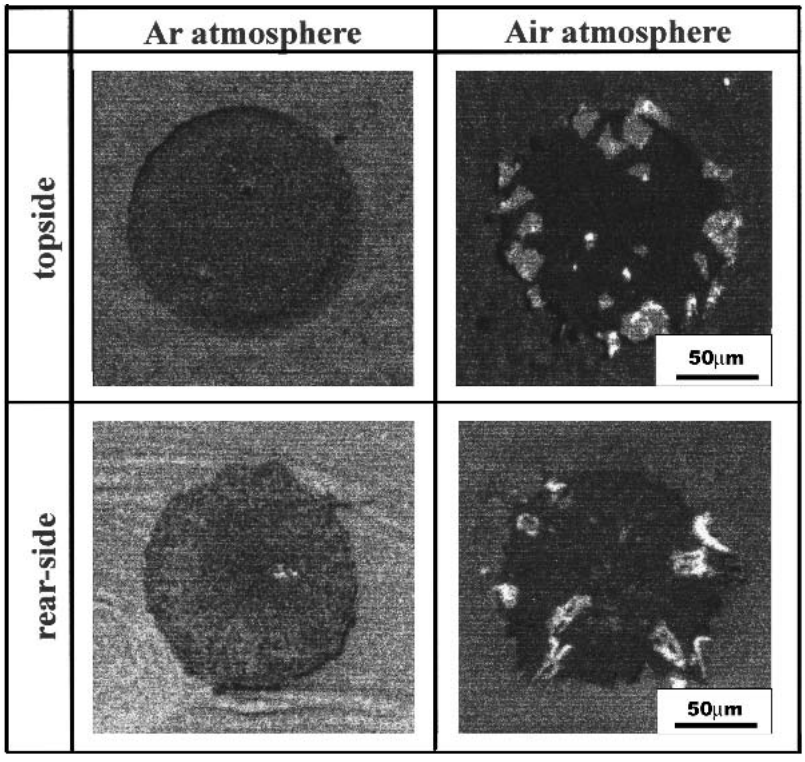

Fig. 6 Oxygen K_α images of topside and rear-side of cast iron splats sprayed at P_C = 100 kPa in Ar and air atmosphere

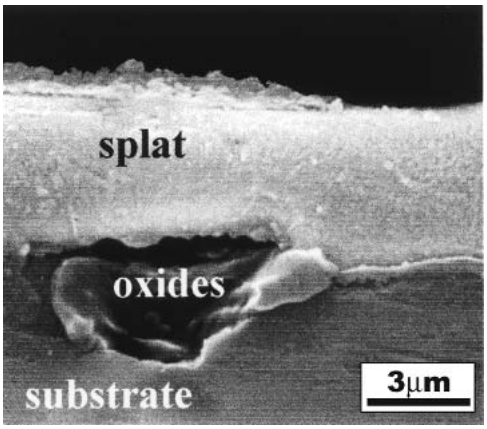

Fig. 7 SEM micrograph showing a cross section of cast iron splat sprayed at P_C = 100 kPa in air atmosphere

mosphere, the number fraction of removed splats slightly increases with P_C, while the number fraction of those sprayed in air atmosphere greatly increases with P_C. The number fraction of removed splats sprayed in air atmosphere at 100 kPa shows the highest value, that is, the weakest splat adhesion. Spraying in Ar atmosphere obviously improves the adhesive strength of splats. Weak splat adhesion at high P_C is partially linked to pore formation at the interface, as will be discussed later.

3.3 Splat Oxidation

By EPMA, the top side and rear side of cast iron splats sprayed at 100 kPa in Ar and air atmospheres were examined as shown in Fig. 6 of O K_α images. Big oxide zones, which are areas of oxides with diameters range of 5-20 μm, are mainly composed of $FeAl_2O_4$ as identified by XRD and appear on the surface and rear-side of splats sprayed only in air atmosphere. On the other hand, no big oxide zones are detected on the surface and rear-side of splats sprayed in Ar atmosphere. XRD patterns exhibit an increase in $FeAl_2O_4$ intensity with P_C in air atmosphere. Splat oxidation strongly depends on the quantity of absorbed oxygen and on droplet temperature. At high P_C, the flying droplets have lower velocities and are surrounded by many oxygen molecules. These factors promote splat oxidation during flight and impinging on the substrate. For example, the oxygen partial pressure (P_{O2}) is 0.38 kPa in Ar atmosphere at the beginning of spraying, whilst the P_{O2} changes from 5.3 kPa at P_C = 26.3 kPa to 20.9 kPa at P_C = 100 kPa in air atmosphere. Droplets exposed to small amounts of oxygen for a very short dwelling time are not severely oxidized, so that spraying in Ar atmosphere decreases the possibility of splat oxidation.

To obtain a better understanding of the interface and of how these oxides come in contact with the splat and the substrate, a cross-section of splats sprayed at 100 kPa in air atmosphere was examined as illustrated in Fig. 7. The big oxides appear inside splats and are attached to the substrate surface or even engrossed within the substrate. The adhesive strength of splats decreases with an increase in the amount of these oxides due to their brittleness. EPMA line analyses on the cross-sections of splats sprayed at P_C of 100 kPa in Ar and air atmosphere are shown in Fig. 8, which were carried out without crossing the big oxides. Al-

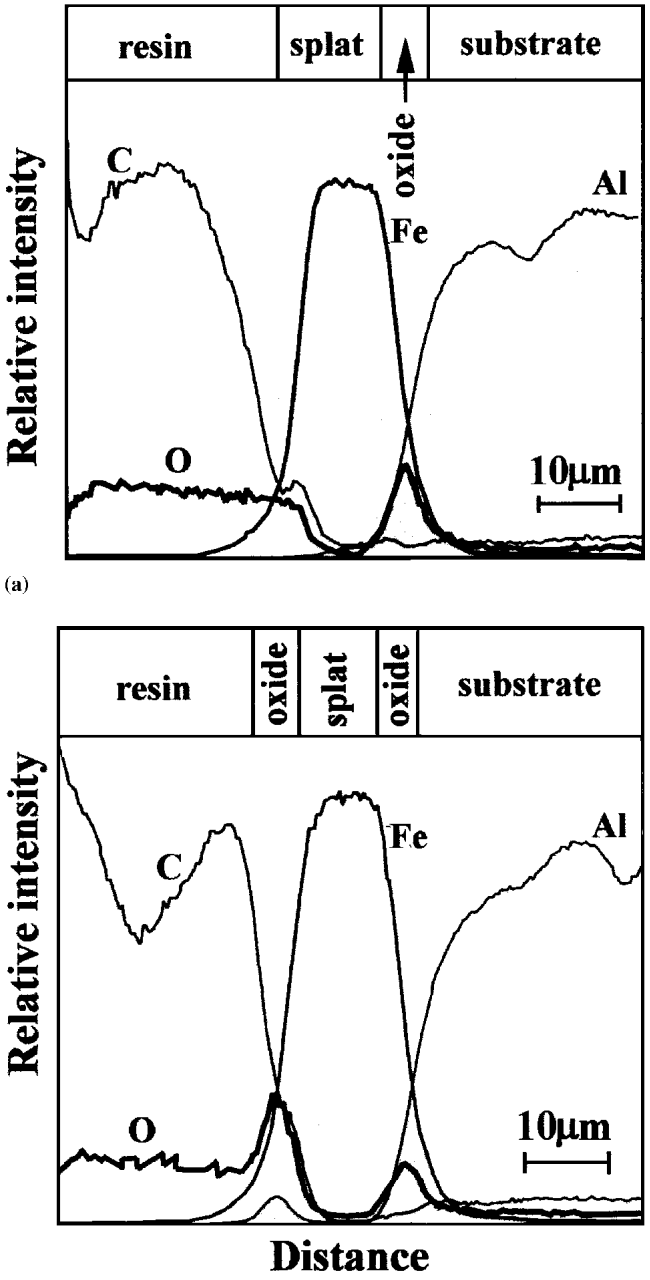

Fig. 8 Elements distribution on splat cross section sprayed at P_C = 100 kPa in **(a)** Ar and **(b)** air atmosphere

though the P_{O2} is 55 times higher in air atmosphere than that in Ar atmosphere at 100 kPa, the splat/substrate interface is slightly oxidized in both cases. Oxidation is also recognized at a splat surface sprayed in air atmosphere. It is worth noting that the weak Al-Kα intensity is recognized at the top side of splats sprayed in air atmosphere. At high P_C in air atmosphere, the droplets velocities are rather low and thus they are exposed for longer time to the atmospheric oxygen, which promotes the oxidation process during flight. At the interface, mutual diffusion of a melted substrate with droplets occurs, and the thin-layered $FeAl_2O_4$ is formed, besides big oxides.

The substrate surface was examined after removing splats sprayed at 46.7 kPa in Ar and at 100 kPa in air atmosphere, as shown in Fig. 9. There exists a thin oxide layer on the remained substrate surface in both cases. This thin oxide layer exhibits higher adhesion to the substrate than the splat. Big holes, which seem to be the location of removed big oxides, are included in the thin oxide layer left after removing splats sprayed in air atmosphere. The attachment of these big oxides to the splat rear-side was identified by EPMA as shown in Fig. 6.

3.4 Ridge Formation

Deformed substrate ridges were observed by examining the periphery of the cross-sections of cast iron splats sprayed at different P_C as illustrated by SEM images in Fig. 10. A small ridge is observed adjacent to the splat periphery sprayed at low P_C of 26.3 kPa, whereas there are no ridges detected for splats sprayed at high P_C. The ridge formation results from not only the plastic deformation of the substrate as a result of the kinetic energy upon impact but also the movement of partially melted substrate surface during the flattening of cast iron droplet. The interfacial temperature (T_i) calculated in the previous work[6] at T_S of 473 K exceeds the melting point of the substrate material, which leads to partial surface melting upon impinging. The ridge formation is characterized by spraying of high melting point materials on a low melting point substrate. Upon impinging and during droplet flattening, the heat transfer from the droplet to the substrate causes the substrate surface to melt, and mutual diffusion occurs at the interface, which eases the thin oxide layer formation of $FeAl_2O_4$. The ridge formation can be considered as a kind of mechanical bond, which also improves the adhesion property of splats. This observation proves the importance of the first deposited layer in the adhesion property of coatings.

3.5 Solidification Rate and Splat Microstructure

Now we will discuss the correlation between splat microstructure and solidification rate based on the temperature gradient within a flat disk cast iron splat. The heat flux into the splat/substrate interface from the splat is equated to the flux away from the interface into the substrate. The general differential equation for heat conduction is described by Eq 2 in the case of one-dimensional heat flow with no interface thermal resistance:

$$dT/dt = (k/\rho C_p)d^2T/dt^2 \quad \text{(Eq 2)}$$

The substrate is semi-infinite in the negative x-domain with an interfacial temperature of T_i, which is determined by the thermal properties of both the splat and substrate as listed in Table 2.[16] Assuming the preheat substrate temperature to be T_S and the molten splat temperature to be T_d, after some solidification has occurred in the cast iron splat, the solution of the temperature gradient within the splat is given by Eq 3[17]:

$$(T - T_i)/(T_d - T_i) = \text{erf}[x/2(k't/\rho' C_p')^{1/2}] \quad \text{(Eq 3)}$$

According to the Geiger and Poirier's method,[16] T_i is calculated through assuming the droplet temperature (T_d = 2383 K) measured by Sodeoka et al.[7] The T_d is almost constant at a certain spray distance regardless of the chamber pressure (P_C), while the droplet velocity decreases with an increasing P_C. Then the effect of superheat (ΔT) on the solidification time must add to the absorbing latent heat of molten cast iron. Taking into account the total quantity of heat to be removed from the molten splat and assuming no difference in the density of the liquid and solid cast iron, the effective heat of fusion can be expressed by the sum of latent heat of fusion and the liquid's superheat:

$$H_f' = H_f + C'_{P(\text{liquid})}\Delta T \quad \text{(Eq 4)}$$

The calculated T_i is 1570 K in all P_C, which exhibits that the substrate surface is partially melted. Note that the solidification time is proportional to the square of the splat thickness (x_o). At P_C = 26.3 kPa the average x_o is 1.96 μm, and 2.59 μm at P_C = 100 kPa in Ar atmosphere. From this information we can estimate

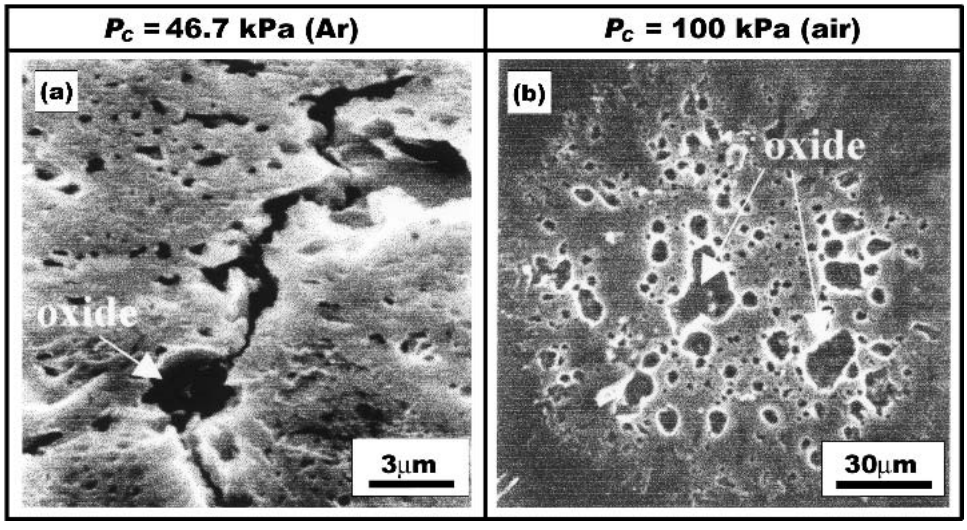

Fig. 9 SEM micrographs showing a substrate surface after removing splats

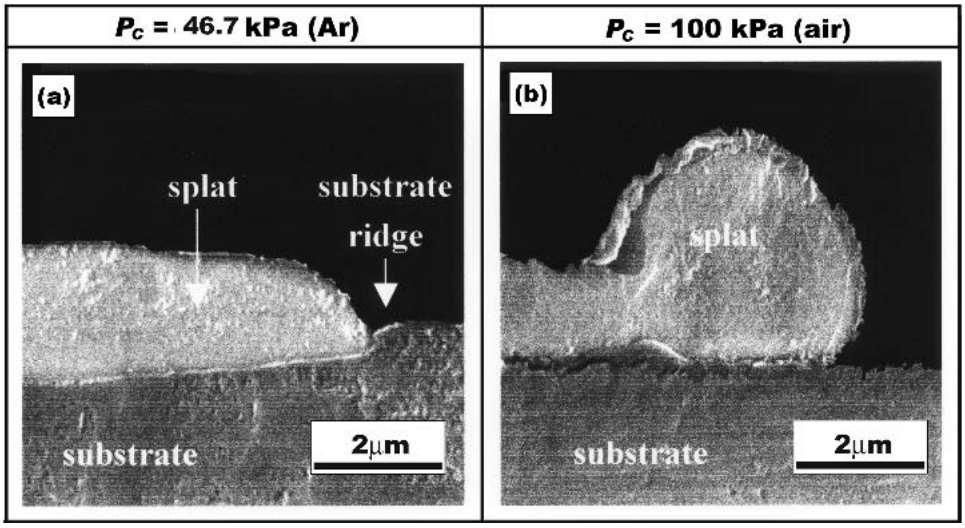

Fig. 10 SEM micrographs showing a cross section of splat peripheries

Table 2 Physical Properties of Cast Iron Splat and Aluminum Alloy Substrate

Property	Cast Iron Splat	Al-Si-Cu Substrate
Thermal conductivity, J/m K s	$k' = 33$	$k = 150$
Solid density, kg/m^3	$\rho' = 7300$	$\rho = 2740$
Specific heat, J/kg K	$C_P' = 670$	$C_P = 1100$
	C_P' (1) = 963	…
Heat of fusion, kJ/kg	$H_f = 210$	…
Melting point, K	$T_M = 1423$	$T_{Al} = 853$

the solidification time of the splat, as described in Fig. 11 as a function of x_o^2. The numerical calculations of solidification time with different x_o show an increase in the splat solidification time with an increasing P_C.

With XRD analyses, the splats are composed of Fe-Si-C, Fe_3C, α-Fe, $FeAl_2O_4$, and graphite, though each diffraction intensity varies with P_C. The top sides of cast iron splats were polished and etched for microstructural evaluation, as shown in Fig. 12, of splats sprayed at different P_C in Ar and air atmosphere. Microstructures of cast iron splats are related to P_C through a change in the solidification time. As mentioned earlier, the solidification time increases as P_C increases, due to a decrease in the droplet velocity and thus an increase in the splat thickness. Consequently, a rapidly solidified Fe-Si-C phase appears with high intensity in the case of spraying at low P_C. In contrast, the intensity of Fe-Si-C decreases, whereas graphite, Fe_3C, α-Fe, and $FeAl_2O_4$ increase as the solidification rate decreases. In the extreme case, splats sprayed in air atmosphere are prone to form internal oxides, as shown in Fig. 12(c).

Thermal resistance at the splat/substrate interface was ignored in the above discussion; however, it becomes rather important at high P_C, especially in air atmosphere, due to an oxidized substrate surface. The interface resistance makes the solidification rate and the T_i decrease, which causes a change in the splat microstructure and also prevents splats from the formation of deformed ridges.

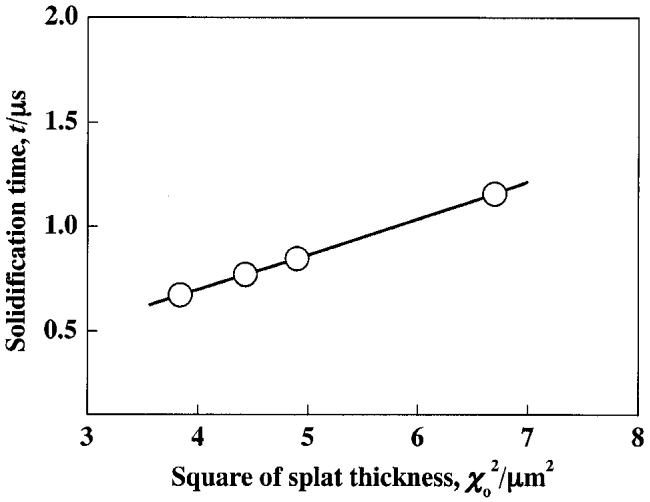

Fig. 11 Change in solidification time of superheated cast iron splat as a function of x_o^2

4. Conclusion

The effects of chamber pressure (P_C) on the morphology, oxidation and microstructure of cast iron splats on a mirror polished aluminum alloy substrate were examined as a fundamental study on plasma sprayed cast iron coatings. The following results were obtained:

1) There exist two different types of splat morphologies: mainly disk-type splats at low P_C and star-shaped splats at high P_C. At the interface, there appear many pores sprayed at high P_C, which weaken the adhesive strength.
2) Big oxide zones composed of $FeAl_2O_4$, which also reduce the adhesive strength, are observed at the interface of splats sprayed at high P_C in air atmosphere. However, no big oxides appear in splats sprayed in Ar atmosphere, so the oxide formation is mainly due to the reaction with atmospheric oxygen.

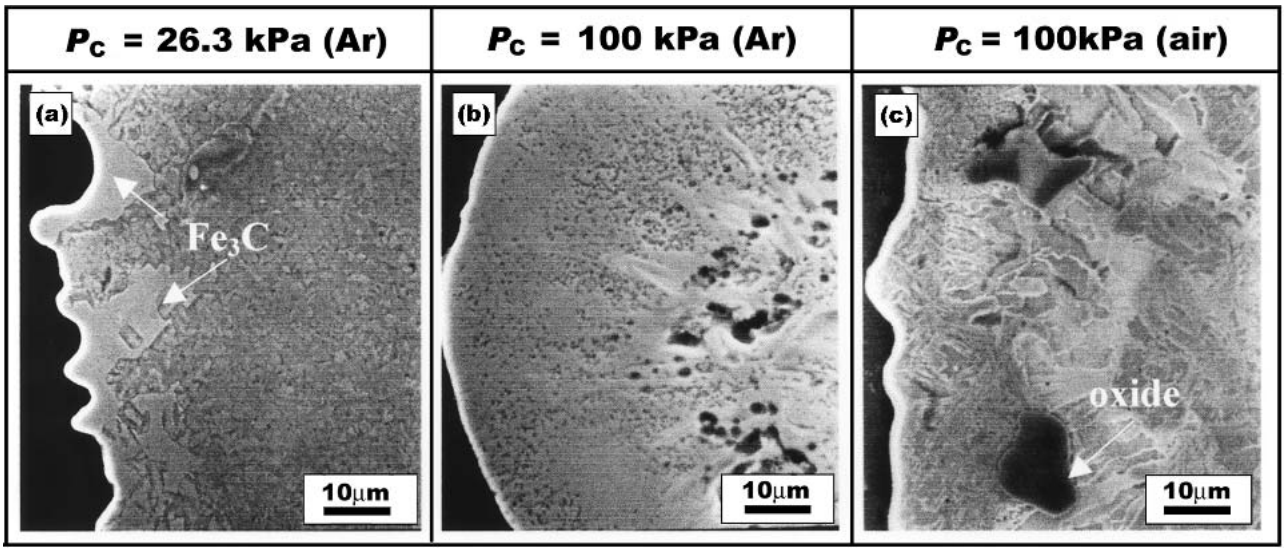

Fig. 12 SEM micrographs showing a polished and etched topside of cast iron splats sprayed at different P_C

3) Small deformed substrate ridges, mainly due to the partial melting of the substrate surface, are formed adjacent to the splat periphery sprayed at low P_C. No ridges are observed at high P_C of 100 kPa because of lowering the interfacial substrate temperature due to the thermal resistance.
4) Splat microstructure is greatly influenced by P_C, because it affects the splat thickness and thus the solidification time. Short solidification time in low P_C forms the Fe-Si-C phase, while it prevents cast iron splats from the graphite formation.

Acknowledgments

The present work was partially supported by the Grants-in-Aid for Scientific Research (12450306), Japan and by Grants-in-Aid for Academic Frontier Center from the Ministry of Education, Science, Sports and Culture, Japan.

References

1. M. Ebisawa, T. Hara, T. Hayashi, and H. Ushio: "Production Process of Metal Matrix Composite (MMC) Engine Block," SAE Tech Paper Series, 910835, 1991.
2. K. Funatani, K. Kurosawa, P.A. Fabiyi, and M.F. Puz: "Improved Engine Performance via Use of Nickel Ceramic Composite Coatings," SAE Tech. Paper Series, 940852, 1994.
3. G. Wuest, G. Barbezat, and S. Keller: "The Key Advantages of the Plasma-Powder Spray Process for the Thermal Spray Coating of Cylinder Bores in Automotive Industry," SAE Tech. Paper Series, 970016, 1997.
4. K. Murakami, T. Okamoto, Y. Miyamoto, and S. Nakazono: "Rapid Solidification and Self-annealing of Fe-C-Si Alloys by Low Pressure Plasma Spraying," *Mater. Eng. Sci., A117,* 1989, pp. 207-14.
5. R.C. Dykhuizen: "Review of Impact and Solidification of Molten Thermal Spray Droplets," *J. Therm. Spray Technol*., 1994, *3*(4), pp. 351-61.
6. M.F. Morks, Y. Tsunekawa, M. Okumiya, and M.A. Shoeib: "Splat Morphology and Microstructure of Plasma Sprayed Cast Iron With Different Preheat Substrate Temperature," *J. Thermal Spray Technol*., 2002, *11*(2), pp. 226-32.
7. S. Sodeoka, M. Suzuki, and T. Inoue: "Control of Plasma Sprayed Particle Temperature and Velocity by Chamber Pressure" in *Proc. Int. Thermal Spray Conf.* ASM International, Materials Park, OH, 2001, pp. 737-41.
8. S. Fantassi, M. Vardelle, A. Vardelle, and P. Fauchais: "Influence of the Velocity of Plasma Sprayed Particles on Splat Formation," *J. Therm. Spray Technol*., 1993, *2*(4), pp. 379-84.
9. R. McPherson: "The Relationship Between the Mechanism of Formation, Microstructure and Properties of Plasma Sprayed Coatings," *Thin Solid Films*, 1981, *83,* pp. 297-310.
10. V. Palka, M. Brezovsky, J. Ivan, and J. Sith: "Identification of Oxides in Plasma Sprayed APS Coating of the NiCrAlY Type" in *Thermal Spray: International Advances in Coatings Technology,* C.C. Berndt, ed., ASM International, Materials Park, OH, 1992, pp. 537-42.
11. V.V. Sobolev and J.M. Guilemany: "Flattening of Droplets and Formation of Splats in Thermal Spraying: A Review of Recent Work, Part 1," *J. Therm. Spray Technol*., 1999, *8*(1), pp. 87-101.
12. O.P. Solonenko: "The Fundamental Thermophysical Problems of Plasma-Spraying" in *Thermal Spray: International Advances in Coatings Technology,* C.C. Berndt, ed., ASM International, Materials Park, OH, 1992, pp. 787-92.
13. J.M. Houben: "Future Development in Thermal Spraying" in *Proc. 2nd Natl. Conf. Thermal Spray,* Long Beach, CA, ASM International, Materials Park, OH, 1985, pp. 1-12.
14. M.P. Planche, O. Betoule, J.F. Coudert, A. Grimaud et al.: "Performance Characteristics of a Low Velocity Plasma Spray Torch" in *Thermal Spray Coatings: Research, Design and Applications,* C.C. Berndt, ed., ASM International, Materials Park, OH, 1993, pp. 81-87.
15. V.V. Sobolev and J.M. Guilemany: "Influence of Wetting and Surface Effects on Splat Formation During Thermal Spraying," *Mater. Lett*., 1998, 37, pp. 132-37.
16. E.A. Brandes and G.B. Brook: in *Smithells Metals Reference Book,* 7th ed., Butterworth-Heinemann, Oxford, UK, 1992.
17. G.H. Geiger and D.R. Poirier: in *Transport Phenomena in Metallurgy,* Addison-Wesley, Reading, MA, 1973, pp. 329-60.